PRAMANA
— journal of
physics

Vol. 61, No. 2
August 2003
pp. 447–454

Structures of some surfactant–polyelectrolyte complexes

REMA KRISHNASWAMY[1], V A RAGHUNATHAN[1] and A K SOOD[2]
[1]Raman Research Institute, C. V. Raman Avenue, Bangalore 560 080, India
[2]Department of Physics, Indian Institute of Science, Bangalore 560 012, India

Abstract. Structures of complexes formed in aqueous solutions by some anionic polyelectrolytes (double and single stranded (ds and ss) DNA, poly(vinyl sulfonate) (PVS), and poly(styrene sulfonate) (PSS)) with a cationic surfactant system consisting of cetyltrimethylammonium bromide (CTAB) and sodium 3-hydroxy-2-naphthoate (SHN) have been determined using small angle X-ray diffraction. All complexes are found to have a two-dimensional (2-D) hexagonal structure at low SHN concentrations. Analysis of the diffraction data shows that the ds DNA–CTAB complex has an intercalated structure, with each DNA strand surrounded by three cylindrical micelles. On increasing SHN concentration, DNA–CTAB–SHN complexes exhibit a hexagonal-to-lamellar transition, whereas PVS complexes show a hexagonal $\rightarrow$ centered rectangular $\rightarrow$ lamellar transition. PSS complexes show yet another sequence of structures. These results indicate the significant influence of the chemical nature of the polyelectrolyte on the structure of the complexes.

Keywords. Surfactant solutions; polyelectrolytes; DNA.

PACS Nos 61.30.Eb; 61.10.Eq; 87.15.By

1. Introduction

Polyelectrolytes form complexes with oppositely charged surfactants in aqueous solutions, which are of considerable interest due to their potential industrial and biomedical applications [1]. A significant fraction of the counter-ions of a highly charged polyelectrolyte is condensed on to the polymer chain in solution [2]. These as well as the condensed surfactant counter-ions are released on complexation. The resultant increase in the translational entropy of the counter-ions is the main driving force for the formation of these complexes [3]. Complexes of ds DNA with double-tailed cationic lipids have been studied in detail using X-ray diffraction. These systems are found to exhibit either a lamellar or a 2-D hexagonal phase depending upon the lipids used [4,5]. The diffraction pattern of the lamellar phase is consistent with an intercalated structure, with the DNA strands sandwiched between lipid bilayers. The hexagonal phase consists of close-packed inverted cylindrical micelles, with the DNA strands confined in their aqueous cores. A variety of structures has also been observed in complexes of polyelectrolytes with single chain surfactants. Depending on the surfactant concentration and the flexibility of the polyelectrolyte, they are found to form either cubic or hexagonal structures [6–8].

Here we present results of small angle X-ray diffraction studies on mixed surfactant–polyelectrolyte complexes; some of the results on DNA–polyelectrolyte complexes have

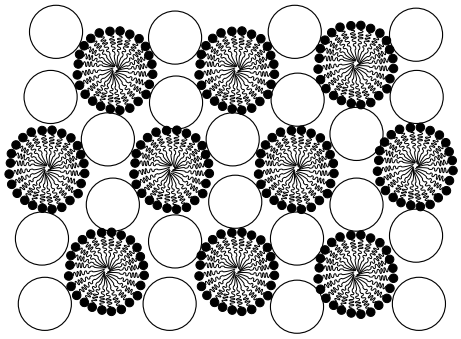

Figure 1. Schematic diagram of the intercalated hexagonal phase, where each DNA strand (denoted by the open circles) is surrounded by three cylindrical micelles. The lattice parameter, $a = \sqrt{3}(R_{\mathrm{m}} + R_{\mathrm{DNA}})$, where R_{m} is the radius of the cylindrical micelle ($\sim$ 2.0 nm) and R_{DNA} that of a hydrated DNA strand ($\sim$ 1.25 nm).

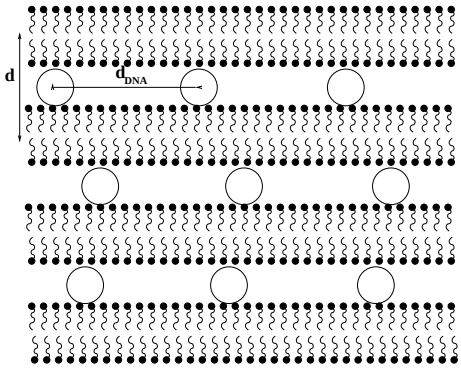

Figure 2. Schematic diagram of the lamellar phase of DNA–surfactant complexes, where the DNA strands are sandwiched between surfactant bilayers.

recently been published [9]. The surfactant system used is a mixture of the single-chained surfactant CTAB, which forms cylindrical micelles in dilute solutions [10], and SHN. The addition of SHN to CTAB is known to lead to a cylinder to bilayer transformation of the surfactant aggregates at a relative SHN concentration, α (=[SHN]/[CTAB]) ~ 0.64 [11]. Complexes of all the three polyelectrolytes have a hexagonal structure at lower values of α. Analysis of diffraction data from ds DNA–CTAB complex shows that it has an intercalated hexagonal structure, where each DNA strand is surrounded by three cylindrical micelles (figure 1). At higher α a lamellar complex is obtained in the case of DNA, whose structure is similar to that found in the case of double-chained lipids (figure 2). In PVS complexes we find a hexagonal $\rightarrow$ centered rectangular $\rightarrow$ lamellar transition on increasing α. PSS complexes exhibit a primitive rectangular structure for intermediate values of α; at higher α another structure is formed, which has not yet been identified. These results indicate that the chemical nature of the polyion is an important parameter in determining the structure of the complexes.

2. Experimental

Sodium salts of calf thymus ds DNA (30–50 kbp) was purchased from Sigma. CTAB, 3-hydroxy-2-naphthoic acid (HNA), and sodium salts of PVS and PSS (MW=70000) were obtained from Aldrich. M13 mp 18 ss DNA (7250 bp) was obtained from Bangalore Genei. Sodium salt of HNA was prepared by adding equivalent amounts of NaOH to the acid solution. Other chemicals were used as received. The surfactant solutions were prepared in deionized water (Millipore), with the relative SHN concentration, α, varying from 0 to 0.7. The complexes precipitated out immediately on adding the polyelectrolyte to the surfactant solution. They were taken in glass capillaries along with some of the supernatant for X-ray diffraction studies. The relative concentration of the polyelectrolyte, ρ = (weight of CTAB)/(weight of polyelectrolyte), was varied over a wide range about the isoelectric point, ρ_{iso}, where the positive charges of the CTA^+ ions are balanced by the HN^- ions and the negative charges on the polyelectrolyte. Cu K_α radiation from a rotating anode X-ray generator (Rigaku, UltraX 18) operating at 50 kV and 80 mA was used to produce the diffraction patterns, which were collected on an image plate (Marresearch).

3. Results and discussion

3.1 *DNA–CTAB–SHN complexes*

These are found to be birefringent under a polarizing microscope. Diffraction pattern of the ds DNA–CTAB system shows three peaks in the small angle region (figure 3). The magnitudes of their scattering vectors, q, are in the ratio $1:\sqrt{3}:2$, corresponding to the (1,0), (1,1) and (2,0) reflections from a 2-D hexagonal lattice with lattice parameter $a = 5.64 \pm 0.09$ nm. The peak positions and their relative intensities are independent of ρ and CTAB concentration up to 300 mM. There are two possible ways of packing DNA strands and CTAB micelles in a 2-D hexagonal lattice, one of which is the intercalated phase shown in figure 1, and the other is the inverted hexagonal phase seen in some DNA–lipid complexes [5]. Neither of them can be ruled out on the basis of the observed values of a.

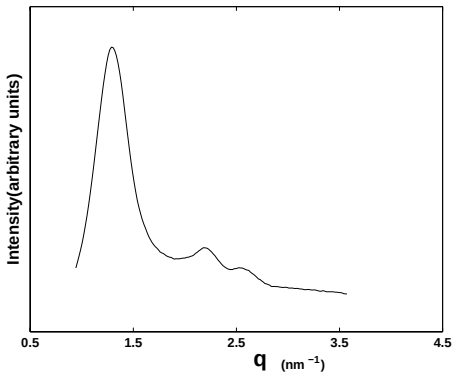

Figure 3. Diffraction pattern of DNA–CTAB complex at $\rho = 7.2$.

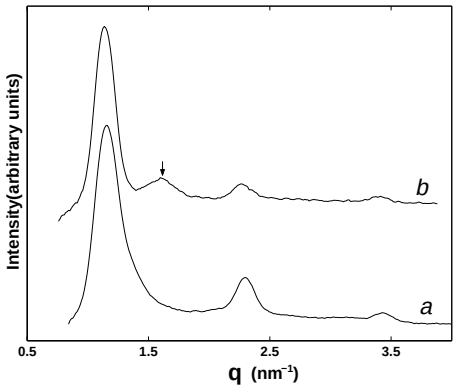

Figure 4. Diffraction patterns of DNA–CTAB–SHN complexes at $\alpha = 0.7$. Curves (a) and (b) correspond to $\rho = 14.4$ and 3.0, respectively. The arrow on curve (b) indicates in-plane DNA–DNA correlation peak. $\rho_{iso} = 3.74$ at $\alpha = 0.7$.

The hexagonal phase persists in the presence of SHN, with a increasing gradually to 6.06 nm at $\alpha = 0.55$. For $\alpha > 0.6$ a lamellar complex is obtained (figure 4a and b).

In order to determine the structure of the hexagonal phase, we have carried out detailed analysis of the diffraction data. Models for the electron density, $\rho(x,y)$, in a plane normal to the axis of the cylindrical micelles in the two possible structures were constructed and their diffraction patterns were calculated. In these models, the DNA strand was represented as a circular disc of uniform electron density ρ_D. Note that ρ_D has contributions not only from the atoms in the DNA molecule, but also from water molecules and counter-ions present in the solution. The radius r_D of this disc was taken to be that of a DNA molecule with a hydration shell around it (1.25 nm). Each cylindrical micelle was represented as a circular disc of electron density ρ_c and radius r_c corresponding to the chain region, surrounded by an annular ring of density ρ_h and width r_h corresponding to the headgroup region. The inverted micelle was modeled as an annular ring of density ρ_h and width r_h, corresponding to the headgroup region, surrounding the circular disc representing the DNA molecule. Values of ρ_c, ρ_h, ρ_w (electron density of water), r_c, and r_h were taken from the literature [12]. Because of the different contributions to ρ_D, mentioned earlier, it could not be estimated. Therefore, the relative intensities of the (1,1) and (2,0) reflections with respect to that of the (1,0) reflection were calculated from the two models for a reasonable range of values of ρ_D (figure 5). As can be seen from the figure, only in the case of the intercalated hexagonal phase the calculated and observed intensities match for a particular value of ρ_D, thus confirming this structure. As mentioned earlier, DNA–CTAB–SHN complexes exhibit a hexagonal-to-lamellar transition near the value of α at which the surfactant aggregates show a cylinder-to-bilayer transformation. This implies that the shape of the surfactant aggregates in the complexes is the same as that in the surfactant solution. Therefore, this observation also supports the intercalated structure, where each DNA strand is surrounded by three cylindrical micelles (figure 1).

Structure of the lamellar DNA complex is similar to that found in DNA–lipid systems, with a periodicity of ~ 5.5 nm (figure 2) [4]. At DNA concentrations below the isoelectric point ($\rho_{iso} = 2.81$ at $\alpha = 0.6$), we could not observe a peak corresponding to the DNA–DNA separation in the bilayer plane, probably due to its proximity to the strong first-order

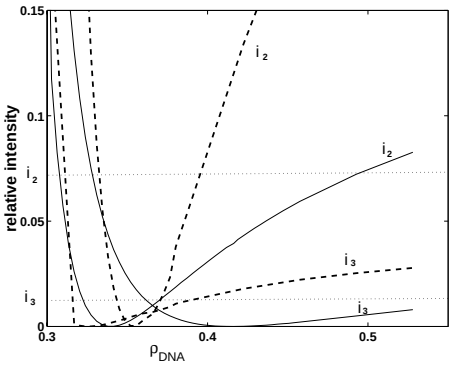

Figure 5. Variation of the relative intensities of the (1,1) (i_2) and (2,0) (i_3) reflections with respect to that of the (1,0) reflection, with ρ_D. The dashed lines correspond to the intercalated hexagonal model and the solid ones to the inverted hexagonal model. The dotted lines correspond to the observed values. Note that only in the case of the inverted hexagonal model the calculated intensities match with the observed ones for a particular value of ρ_D.

lamellar peak (figure 4a). However, at higher DNA concentrations it is clearly seen in the diffraction pattern (figure 4b). Our observations are consistent with a rapid change in the DNA–DNA spacing near the isoelectric point, as found in DNA–lipid complexes [13].

ss DNA complexes also show a hexagonal phase at lower values of α and a lamellar phase at higher α. The lattice parameters in this case are only about 0.5 nm less than those in the case of ds DNA complexes.

3.2 *PVS–CTAB–SHN complexes*

These complexes are also birefringent and diffraction pattern of the SHN-free complex corresponds to a 2-D hexagonal lattice, with $a = 4.64 \pm 0.08$ nm (figure 6a). The hexagonal phase is stable up to $\alpha \sim 0.4$. a increases gradually with SHN concentration and is equal to 5.16 ± 0.08 nm at $\alpha = 0.4$. For values of α in the range 0.4–0.7, a 2-D centered rectangular lattice (cmm) is obtained (figure 6b), with lattice parameters $a = 11.34$ nm and $b = 4.74$ nm. Interestingly, for $\alpha > 0.7$ a lamellar phase is obtained with a spacing of 4.34 nm (figure 6c).

3.3 *PSS–CTAB–SHN complexes*

These also form a hexagonal phase at low SHN concentrations (figure 7a). As in other cases, a increases with α, from 4.64 nm at $\alpha = 0$ to 5.05 ± 0.05 nm at $\alpha = 0.2$. For α between 0.4 and 0.6 the peaks in the diffraction patterns (figure 7b) can be indexed on a rectangular lattice corresponding to the plane group pgg. The lattice parameters a and b vary from 9.34 and 5.36 nm at $\alpha = 0.5$–9.70 and 5.56 nm at $\alpha = 0.6$. At higher SHN concentrations yet another phase is formed, which we have not been able to identify. The

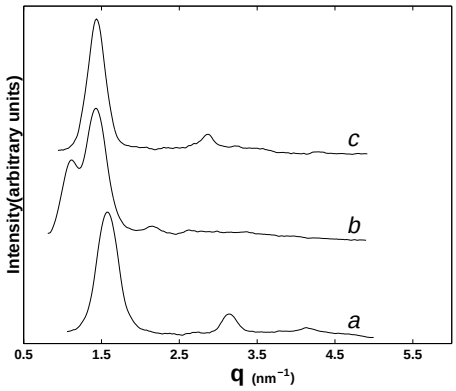

Figure 6. Diffraction patterns of PVS–CTAB–SHN complexes. α and ρ for the different curves are: 0, 1.1 (a); 0.4, 1.1 (b); 0.7, 1.1 (c).

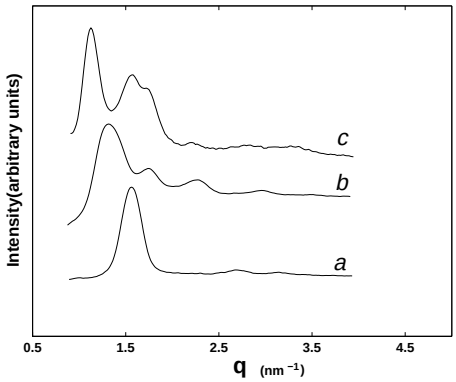

Figure 7. Diffraction patterns of PSS–CTAB–SHN complexes. α and ρ for the different curves are: 0, 1.8 (a); 0.6, 4.5 (b); 0.7, 12.0 (c).

diffraction pattern of this phase shows three peaks in the small angle region without any specific relation between the corresponding q (figure 7c).

The hexagonal phase of PVS and PSS complexes with CTAB–SHN can be expected to consist of cylindrical micelles bridged by polyelectrolyte chains, as in the case of poly(acrylic acid) (PAA)–CTAB complexes [7]. The lattice parameters of the rectangular phase of PVS and PSS complexes do not depend on the polyelectrolyte concentration. Therefore, these structures most probably consist of ribbon-like aggregates arranged on a 2-D rectangular lattice (figures 8 and 9), as found in some surfactant systems in between the hexagonal and lamellar phases [14,15].

4. Conclusions

The complexes formed by some anionic polyelectrolytes in aqueous solutions with a cationic surfactant system have been studied using small angle X-ray diffraction. These complexes are found to show a sequence of structures on changing the surfactant composition.

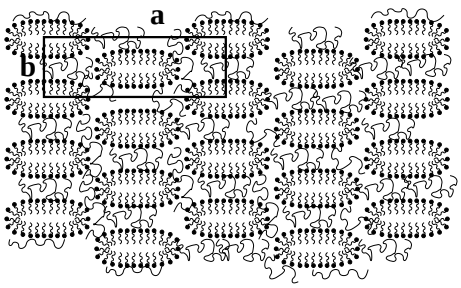

Figure 8. Schematic diagram of the centered rectangular cmm phase seen in PVS complexes at intermediate SHN concentrations, consisting of ribbon-like surfactant aggregates bridged by polymer chains.

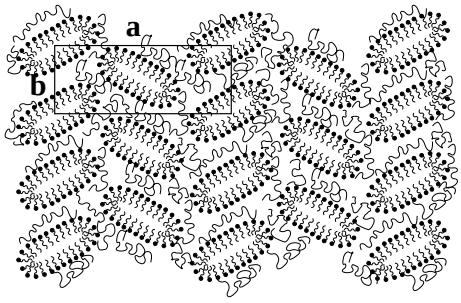

Figure 9. Schematic diagram of the rectangular pgg phase observed in PSS complexes at intermediate SHN concentrations, consisting of ribbon-like surfactant aggregates bridged by polymer chains.

Different structures are also obtained with different polyelectrolytes. The charge densities of all the four polyelectrolytes used are comparable. The persistence length of ss DNA and PVS are $\sim$1 nm, whereas those of ds DNA and PSS are about 50 and 10 nm, respectively. Therefore, differences in the structures obtained with different polyelectrolytes cannot be attributed to differences in the values of these parameters. Hence we may conclude that the results presented here show the importance of specific interactions in the formation of these complexes.

Acknowledgements

We thank Dominique Langevin, M Muthukumar and Sriram Ramaswamy for helpful discussions. AKS thanks K R K Easwaran for his involvement in the early stages of this work.

References

[1] See, for example, *Interactions of surfactants with polymers and proteins* edited by E D Goddard and K P Ananthapadmanabhan (CRC Press, Boca Raton, 1993)
[2] F Oosawa, *J. Polym. Sci.* **23**, 421 (1957)
G S Manning, *J. Chem. Phys.* **51**, 924 (1969)

[3] R Bruinsma, *Euro. Phys. J.* **B4**, 75 (1998)
D Harries, S May, W M Gelbart and A Ben-Shaul, *Biophys. J.* **75**, 159 (1998)
[4] J O Rädler, I Koltover, T Salditt and C R Safinya, *Science* **275**, 810 (1997)
[5] I Koltover, T Salditt, J O Rädler and C R Safinya, *Science* **281**, 78 (1998)
[6] K Thalberg, B Lindman and K Bergfeldt, *Langmuir* **7**, 2893 (1991)
[7] P Ilekti, L Piculell, F Tournilhac and B Cabane, *J. Phys. Chem.* **B102**, 344 (1998)
P Ilekti, T Martin, B Cabane and L Piculell, *J. Phys. Chem.* **B103**, 9831 (1999)
[8] S Zhou, F Yeh, C Burger and B Chu, *J. Phys. Chem.* **B103**, 2107 (1999)
[9] R Krishnaswamy, P Mitra, V A Raghunathan and A K Sood, (to appear in *Europhys. Lett.*)
[10] A Svensson, L Piculell, B Cabane and P Ilekti, *J. Phys. Chem.* **B106**, 1013 (2002)
[11] B K Mishra, S D Samant, P Pradhan, S B Mishra and C Manohar, *Langmuir* **9**, 894 (1993)
K Horbaschek, H Hoffmann and C Thunig, *J. Colloid Interface Sci.* **206**, 439 (1998)
[12] F Reiss-Husson and V Luzzati, *J. Phys. Chem.* **68**, 3504 (1964)
[13] I Koltover, T Salditt and C R Safinya, *Biophys. J.* **77**, 915 (1999)
[14] Y Hendrikx and J Charvolin, *J. Physique* **42**, 1427 (1981)
[15] P Kekicheff and B Cabane, *J. Physique* **48**, 1571 (1987)